Fracture Mechanics of Concrete Structures
Proceedings FRAMCOS-3
AEDIFICATIO Publisher, D-79104 Freiburg, Germany

THREE-DIMENSIONAL FRACTAL ANALYSIS OF MICROSTRUCTURAL MORPHOLOGIES IN CONCRETE

Alberto Carpinteri, Bernardino Chiaia and Stefano Invernizzi
Department of Structural Engineering, Politecnico di Torino,
10129 Torino, Italy.

Abstract

The fracture process in concrete cannot be properly understood in an Euclidean framework, due to its complex morphology at the micro- and meso-level. The inherent flaws interact through a multi-scale process, leading to self-affine fracture surfaces. Furthermore, the network of microcracks possesses non-Euclidean geometrical properties. A new experimental equipment has been developed, which allows the entire fracture surface, or any plane cross section, to be digitised and analysed. This represents an important progress with respect to the study of mono-dimensional profiles. In this paper, the 3D algorithms developed for evaluating the fractal dimension of surfaces and stress-carrying sections are described. The invasive fractal character of the fracture surfaces is confirmed. Moreover, the lacunar fractal character of the stress-carrying cross sections, a priori assumed by Carpinteri (1994), is proved experimentally.

Key words: Fractal geometry, fracture surface, porous microstructure.

1 Introduction

The disordered microstructure of concrete is responsible for many peculiar features of the fracture phenomenon. For example, size effects are not explicable in the classical framework. Pre-existing pores, debonded zones and microcracks, interact with each other in a complex manner. Attempts to describe this behaviour by means of deterministic methods (e.g. continuum mechanics) are deemed to be incomplete if not even misleading. Even the most sophisticated measurement of material properties, coupled with the most powerful computers, would not succeed in the exact (deterministic) modelling of the fracture phenomenon. On the other hand, randomness alone cannot justify the self-organised complexity which comes into play in the fracture of concrete. On the contrary, the invariant features can be put into evidence by approaching the problem from a completely new viewpoint (Carpinteri, 1994).

Cooperative phenomena are nowadays successfully interpreted by means of alternative methods, such as catastrophe theory, fractals, renormalization group and chaos theories. Modelling the microstructure by means of fractal domains permits to capture the hierarchical aspect of damage accumulation and crack propagation. It is nowadays well known that the fracture surfaces of concrete are invasive self-affine fractals over a broad scale range (Mihashi *et al.*, 1995). This implies that the stress-singularity at the tip of a propagating crack is smoothened and the energy is dissipated over a higher dimensional domain. The size effect on fracture energy and the crack-resistance behaviour can both be explained (Carpinteri & Chiaia, 1996). Another aspect of the same problem is represented by the lacunarity of the porous microstructure, which represents a random field explaining the size effect on the nominal tensile strength (Carpinteri, 1994).

In this paper, an innovative experimental methodology is described. By means of a completely automatic laser system, the 3D morphology of the fracture surface can be digitised. The application of the 3D fractal algorithms to these domains confirms the invasive character of the fracture loci. In addition, if planar cross-sections of the virgin material are considered, the pore and void distribution (like the moon-craters distribution) can be easily extracted from the laser-scanned topography. This procedure, which yields the effective depth and shape of the pores, permits to overcome the drawbacks and ambiguities of traditional image analysis techniques, where dark particles often confuse with pores. Several analyses have been carried out, confirming the lacunar fractal character of the ligament. The same investigation allows us to confirm the self-similar character of the pore size distribution, which has been assumed in various statistical models of brittle fracture.

2 Experimental methodology

A new experimental methodology has been developed at Politecnico di Torino, with the purpose of overcoming two major limitations commonly encountered with the existing techniques. First, it allows to acquire the entire three-dimensional surface topography, which is necessary for a real three-dimensional fractal analysis. In the literature, the fractal dimension of surfaces is often calculated only by extrapolating the values of the fractal dimension of vertical sections (profiles) or horizontal sections (in the slit-area method). The relation that links the fractal dimension of a set with that of its subsets is demonstrated only in the case of mathematical fractals, not in the case of natural fractals. The second result is to avoid the ambiguities of traditional image analysis techniques, where dark particles often confuse with pores.

The experimental equipment is sketched in Fig. 1. The specimen to be analysed (Fig. 1f) is rigidly framed into a solid truss. The surface height measurement is performed by means of a Keyence^{TM} LB-12 laser profilometer (Fig. 1g), by counting the number of wave-cycles between the ray emission and the ray reception after the reflection on the specimen surface. The laser is driven by two orthogonal micrometric step-motors (UE30CC: UT 100-100, Fig. 1h), controlled by the MM2000 interface (Newport Klinger^{TM}, Fig. 1d), plugged in an ISA-slot of a PC motherboard (Fig. 1b). The analogical signal provided by the LB-72 laser controller (Fig. 1e) is converted in a 16-bit precision digital signal by the DAQ PC-LPM-16 data acquisition board (National Instruments^{TM}, Fig. 1c). A dedicated software (Fig. 1a) provides extreme versatility and the full automation of the surface acquisition process. The digitised surface can extend over a $50mm \times 100mm$ area, and a maximum precision of $2\mu m$ can be achieved both in vertical and horizontal directions.

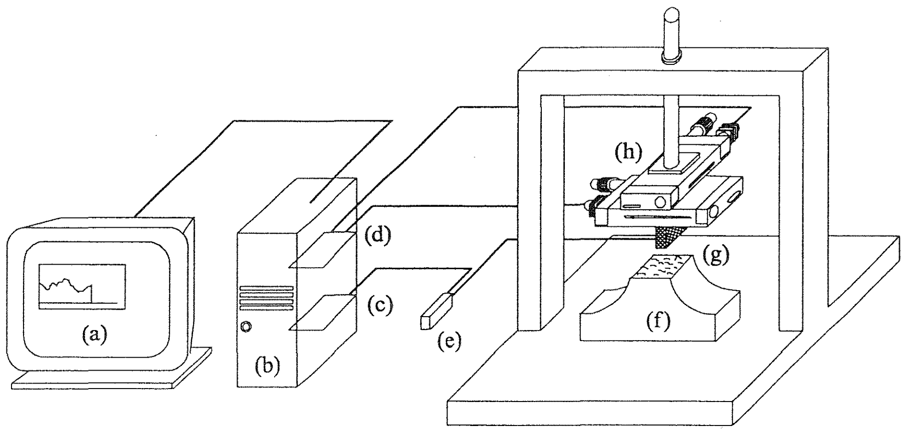

Fig. 1. Experimental equipment: monitor (a), PC case (b), PC-LPM-16 (c), MM2000 (d), LB72 (e), specimen (f), LB12 (g), UE30CC (h).

Several concrete fractured surfaces, after tensile rupture, have been digitised. One of them is shown in Fig. 2a. This surface extends over a $4 \times 4\text{cm}^2$ projection area, and has been stored as a 2048×2048 pixel array. Therefore, a $20\mu m$ step was adopted. It is believed that further refinement is not necessary for the mesostructural characterisation of concrete-like materials. The surface is extremely rough and shows more and more details as the observation resolution increases. The same morphology is observed under different magnifications. This confirms a substantial scale invariance. As it will be shown in the following, the scale-dependent value of the apparent area tends to infinity as the resolution increases. Therefore, it is not consistent to treat this domain as a smooth Euclidean surface.

Furthermore, planar concrete cross sections have been digitised. They were obtained by cross-cutting undamaged specimens. These surfaces appear almost flat, with localised distribution of moon-like craters (Fig. 2b) due to the intersection of the cutting plane with the inherent microstructural voids. Therefore, the effective resistant cross section is less dense and compact than the nominal cross section. In the case of uniform porosity, referring to the nominal cross section does not provide scaling effects. In the real situations, as will be outlined in the following, the porosity is not uniform, and the relative percentage of voids depends on the cross section linear size.

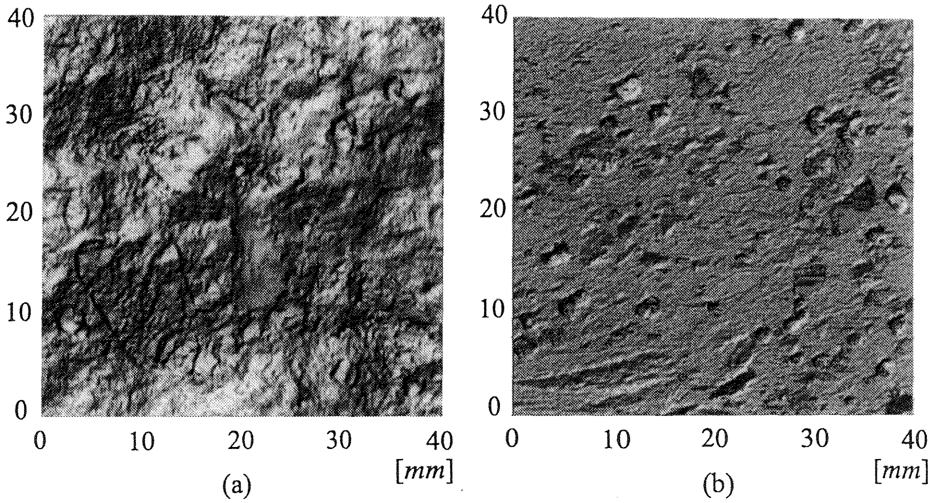

Fig. 2. Shaded reliefs: fracture surface (a), plane cross-section (b).

3 Invasive fractality of fracture surfaces

The digitised fracture surface of concrete has been analysed using three different algorithms and definitions for the fractal dimension calculation. Based on the classical concept of covering dimension, by Mandelbrot (1982), the box-counting method allows to calculate the fractal dimension of lacunar and invasive fractal sets. The fracture surface is assumed to be an invasive self-affine fractal in a statistical sense. This means that a three-dimensional representation of the surfaces $f(x, y, z)$ will be statistically similar to $f(rx, ry, r^H z)$, where r is the scaling factor and H is the Hurst exponent due to the anisotropy in the scaling process.
As shown in Fig. 3, the fractal dimension can be evaluated from the rate of growth of the number N of prisms, necessary to cover the surface, as the size d of the elementary prisms (whose volume is $V = d \times d \times d^H$) decreases. The following equation holds:

$$\Delta_{\mathrm{box}} = \lim_{d \to 0} \frac{\log N}{\log(1/d)}. \tag{1}$$

The fractal dimension of the surface shown in Fig. 2a, calculated according to eq. (1), is equal to $\Delta_{\mathrm{box}} = 2.15$, and confirms the invasive fractal nature of this domain.

While the box-counting algorithm estimates the fractal dimension from the rate of vanishing of the overall covering volume as the reso-

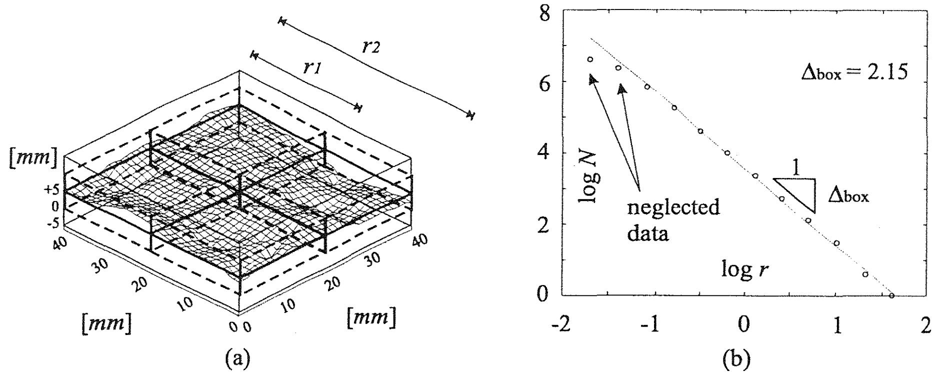

Fig. 3. Box-counting method: covering scheme (a), bilogarithmic diagram (b).

lution increases, the patchwork method approximates the fractal domain by surface elements (Fig. 4a) and the fractal dimension is evaluated from the rate of divergence of the apparent area A (Fig. 4b). In other words, the patchwork method aims at evaluating the same limit value, i.e. the fractal dimension, by approximating it from a different path. For example, if the covering grid size is $r = 20.48mm$, then the apparent area A is equal to $1698.17mm^2$. Increasing the resolution, more and more details are counted and, when $r = 20\mu m$, A becomes equal to $2691.39mm^2$. This confirms the scale dependent nature of fracture surface (Lange & Shah, 1994). The patchwork fractal dimension, originally defined by Clarke (1986), can be computed as:

$$\Delta_{\text{patch}} = 2 - \lim_{r \to 0} \frac{\log A(r)}{\log r}. \tag{2}$$

In Fig 5a, the bilogarithmic diagram $\log A$ versus $\log r$ is shown. The fractal dimension, equal to the slope of the curve, is correctly evaluated only for high resolution (local fractal dimension). On the contrary, it tends to the Euclidean integer value for poor resolution, due to the self-affine character of the surface.

Finally, the fractal dimension of the fracture surface has been calculated by a three-dimensional spectral method, specifically designed for self-affine sets (Turcotte, 1992). It is based on the two-dimensional Fourier Transform, and provides the fractal dimension as a function of the mean spectral power S_{2j} which, for self-affine surfaces, is given by the following power-law:

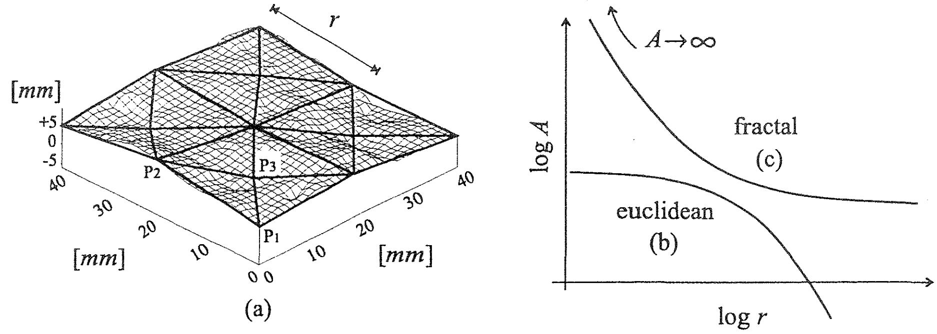

Fig. 4. Patchwork method: triangulation scheme (a), determination of univocal measure for Euclidean sets (b), divergence of the canonical measure for fractal sets (c).

$$S_{2j} = k_j^{-\beta-1}. \tag{3}$$

In eq. (3), k is the radial wave number and β is the slope of the curve in the $\log S_{2j}$ versus $\log k$ bilogarithmic diagram shown in Fig 5b. The spectral fractal dimension can be written as a function of β:

$$\Delta_S = \frac{7-\beta}{2}. \tag{4}$$

The spectral method provides the value $\Delta_S = 2.23$ for the same surface shown in Fig. 2a.

In conclusion, the dimension of this surface should be set in the range $2.15 - 2.29$. Unfortunately, in the case of natural fractals, it is difficult to obtain only one value because the algorithms, although theoretically coincident in the limit, behave differently when applied to real sets.

4 Lacunar fractality of stress-carrying cross sections

In the study of continuous media, we are concerned with the manner in which forces are transmitted through the medium. The Cauchy definition of stress relies on some "regularity" properties (continuity and measurability) of the medium. Experimental investigations show that heterogeneities and defects are present at all the scales in engineering materials and interact with each other in a complex manner. These aspects cannot be neglected when meso- or micro-scales are considered, and in the presence of strain localisation and large stress

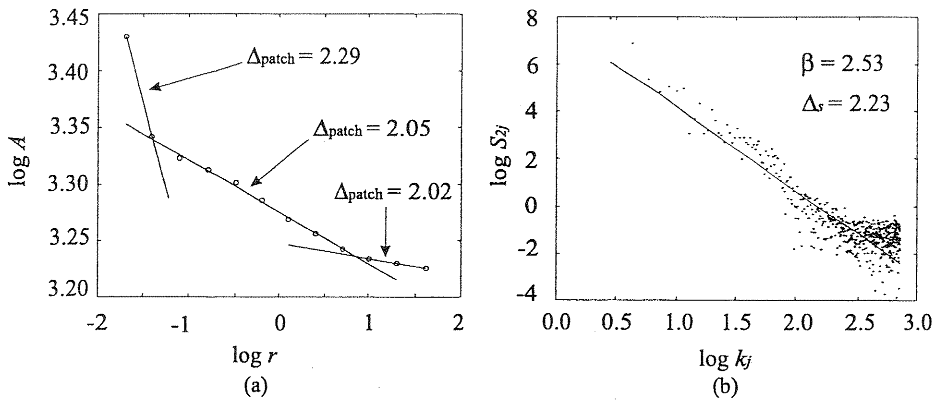

Fig. 5. Bilogarithmic diagrams: patchwork method (a), spectral method (b).

gradients, which is the case of fracture and contact problems. Carpinteri (1994) assumed that the fractal dimension of stressed ligaments in disordered solids were lower than 2.0 due to voids and cracks. Therefore, lacunar domains (possessing a fractal dimension lower than the topologic dimension) can be used to model the stress-carrying cross sections in real materials. The apparent Euclidean measure (length, area or volume) of lacunar sets is scale-dependent and tends to zero as the resolution increases. In these cases, the Cauchy definition of stress can not be applied. The "regularity" properties of the Euclidean sets are lost and are replaced by the non-differentiability. On the other hand, self-similarity comes into play, providing a particular symmetry in the problem (dilatation symmetry). Accordingly, the stress concept needs to be revised and scaling laws must be included (Carpinteri & Chiaia, 1996).

The Menger sponge can be considered as a fractal model for a porous solid. It is shown at the third iteration in Fig. 6a, and its Hausdorff dimension is equal to $\Delta = \log 20/\log 3 = 2.73$. The sponge has zero volume and possesses very peculiar mass properties related to its non-compactness. In fact, if sponges of different linear size are compared, one notes that the nominal density decreases with size according to a non-integer exponent equal to $D-3$. This is confirmed by natural sponges, where the larger the specimen size, the higher the probability of encountering a large hole. Planar cross sections of the Menger sponge are Sierpinski carpets, whose iteration scheme is shown in Fig. 6b. This set presents zero area ($\Delta = \log 8/\log 3 =$

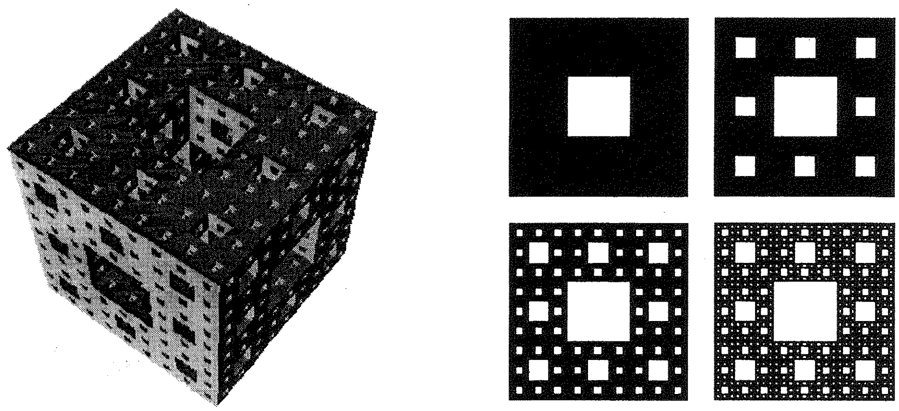

(a) (b)

Fig. 6. Menger sponge (a). Sierpinski carpet iterative generation (b).

1.893) and can be considered as a lacunar cross-section inside a porous medium. In Fig. 2b, an example of a nominal stress-carrying cross-section is shown. It is worth to remind that this lacunar domain is obtained from an undamaged solid. If load had been applied, a larger damage would be present furtherly lowering its compactness.

The true stressed domain is made out of the points that do not belong to the craters, i.e. to the pore structure. Hence, from a theoretical point of view, the actual resisting section can be evaluated by considering the set of points whose heights are exactly equal to the cutting plane height. Practically, the obtained surface (Fig. 2b) is not absolutely plane and presents a low uniform roughness due to the cutting process that can be confused with porosity. For this reason, another virtual plane has been considered, parallel to the cutting section, but at a lower height, which is able to intersect only the real cavities (Fig. 7a). Then, the points, whose height is greater than the virtual plane height, are considered to belong to the real stress-carrying domain, while the remaining points belong to the (complementary) void set. This procedure allows to filter out the noise produced by cutting. However, some information is lost about the finer porosity. To perform the virtual cut, it is also necessary to know the mean real cutting plane by a de-trending algorithm. Fig. 7b shows the resulting cross-section, which can be considered as the real stress-carrying domain.

The fractal dimension of this domain has been calculated using two

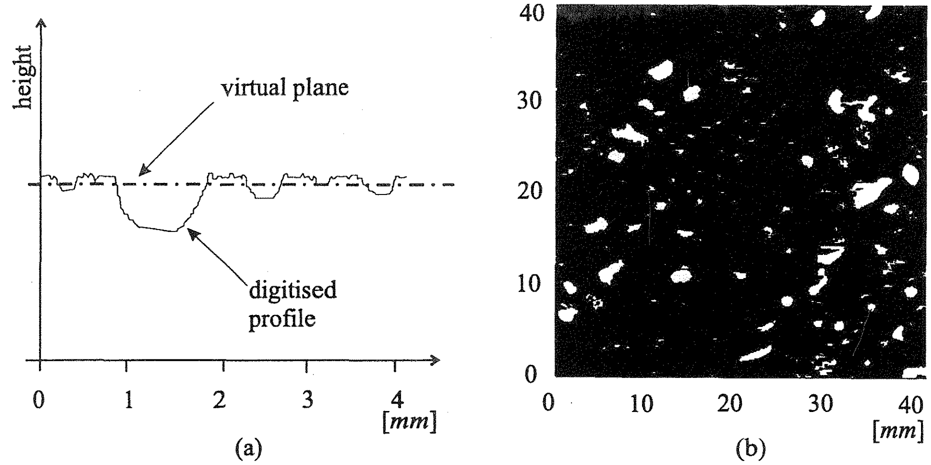

Fig. 7. Virtual plane section scheme (a) and bidimensional map of the effective cross section (b).

different algorithms. At first, the previously introduced box-counting method. The number of boxes needed to cover the set has been calculated for a decreasing value of the size of the square covering element (Fig. 8a). The effective ligament presents a fractal dimension equal to $\Delta_{\text{box}} = 1.96$ (Fig. 8a), which is lower than the integer Euclidean value (equal to 2).

The fractal dimension can be also evaluated by referring to the mass logarithmic density. If the effective cross section were characterised by a uniform distribution of cavities, it would be possible to calculate the density defined as the ratio between the effective area A_{eff} and the nominal area A_{nom}. In the actual case, this density can not be unambiguously calculated because it depends on the resolution and on the size of the considered area. In fact, the complex distribution of the pores causes the probability of finding large cavities to be higher as the size of the considered area increases (like in a natural sponge, Mandelbrot (1982)). The classical density is not constant, but decreases by increasing the nominal size. To obtain a scale-invariant value, it is necessary to refer to the logarithmic density, defined as:

$$\rho_{\log} = \frac{\log A_{\text{eff}}}{\log A_{\text{nom}}}. \tag{5}$$

If d is the linear size of the considered area, the fractal dimension $\Delta_{\log}$ can be evaluated as the limit slope of the bilogarithmic

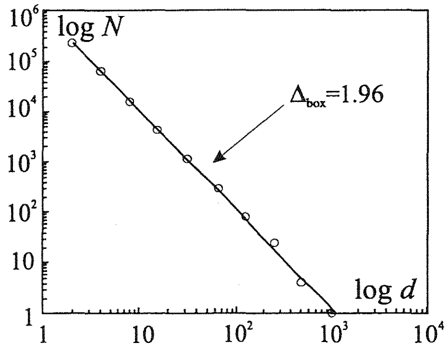

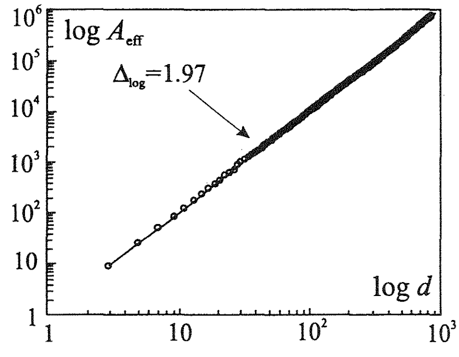

Fig. 8. Bilogarithmic diagram: box-counting method (a), apparent density (b).

diagram ($\log A_{\text{eff}}$ versus $\log d$). In the case of concrete (Fig. 8b), the value $\Delta_{\log} = 1.97$ was determined, in good agreement with the box-counting method.

As a final remark, it is our opinion that this value is too high, even for an undamaged specimen. Higher resolutions should reveal the presence of micro-porosity, which would lower drastically the density and compactness of the stress-carrying domains.

5 Acknowledgements

The present research was carried out with the financial support of the Ministry of University and Scientific Research (MURST), the National Research Council (CNR) and the EC-TMR Contract N^o ERBFM-RXCT 960062.

6 References

Carpinteri, A., (1994) Fractal nature of material microstructure and size effects on apparent mechanical properties. **Mechanics of Materials,** 18, 259-266; also **Internal Report,** Laboratory of Fracture Mechanics, Politecnico di Torino, 1992.

Carpinteri, A. & Chiaia, B., (1996) Power scaling laws and dimensional transitions in solid mechanics. **Chaos, Solitons and Fractals,** 7, 1343-1364.

Clarke, K.C., (1986) Computation of the fractal dimension of topographic surfaces using the triangular prism surface area method. **Computer & Geosciences,** 12, 713-722.

Lange, D.A., Shah, S.P., (1994) Roughness and fracture toughnessof cement-based matrices, in **Size-Scale Effects in the Failure Mechanisms of Materials and Structures** (ed. A. Carpinteri), E.& F.N. Spon, London, 87–96.

Mandelbrot, B.B., (1982) **The Fractal Geometry of Nature.** Freeman, San Francisco.

Mihashi, H., Nomura, N. and Nakamura, H., (1995) What is interpreted from fracture surface in concrete?, in **Fracture Mechanics of Concrete Structures** (ed. F.H. Wittmann), Aedificatio Publishers, Freiburg, 755–768.

Turcotte, D.L., (1992) **Fractal and Chaos in Geology and Geophysics.** Cambridge University Press, Cambridge.